Letter   Editors' Suggestion

Characterizing random-singlet state in two-dimensional frustrated quantum magnets and implications for the double perovskite $Sr_2CuTe_{1-x}W_xO_6$

Huan-Da Ren [1,2], Tian-Yu Xiong,[1] Han-Qing Wu,[3,*] D. N. Sheng,[4,†] and Shou-Shu Gong [1,‡]

[1]*Department of Physics, Beihang University, Beijing 100191, China*
[2]*Department of Physics, Tsinghua University, Beijing 100084, China*
[3]*Guangdong Provincial Key Laboratory of Magnetoelectric Physics and Devices, School of Physics, Sun Yat-Sen University, Guangzhou 510275, China*
[4]*Department of Physics and Astronomy, California State University Northridge, Northridge, California 91330, USA*

Motivated by the experimental observation of a nonmagnetic phase in compounds with frustration and disorder, we study the ground state of a spin-1/2 square-lattice Heisenberg model with randomly distributed nearest-neighbor J_1 and next-nearest-neighbor J_2 couplings. By using the density matrix renormalization group (DMRG) calculation on a cylinder system with a circumference of up to ten lattice sites, we identify a disordered phase between the Néel and stripe magnetic phase with growing J_2/J_1 in the presence of strong bond randomness. The vanished spin-freezing parameter indicates the absence of spin-glass order. The large-scale DMRG results unveil the size-scaling behaviors of the spin-freezing parameter, the power-law decay of the average spin correlation, and the exponential decay of the typical spin correlation, which all agree with the corresponding behavior in the one-dimensional random-singlet (RS) state and characterize the RS nature of this disordered phase. The DMRG simulation also provides insights and opportunities for characterizing a class of nonmagnetic states in two-dimensional frustrated magnets with disorder. We also compare with existing experiments and suggest more measurements for understanding the spin-liquid-like behaviors in the double perovskite $Sr_2CuTe_{1-x}W_xO_6$.

Introduction. A spin liquid (SL) is an exotic quantum liquid state realized in frustrated magnets [1–5], which exhibits long-range entanglement and fractionalized excitations [6–8] and may have potential applications in quantum computation [9]. After an extensive search for decades, spin-liquid-like behaviors have been reported in frustrated antiferromagnets [3–5]. In particular, most of the SL candidates have been characterized as gapless spin-liquid states in experiment [4,10–16]. Nevertheless, theoretical studies have only established SL states in a few highly frustrated models including kagome antiferromagnet and triangular-lattice Heisenberg models with competing interactions [3,5]. Only considering frustrated interactions may be insufficient to account for the widely observed spin-liquid-like behaviors in materials.

Another common factor that may suppress magnetic order is disorder, which naturally exists in materials [11,12,17,18]. In one dimension (1D), the strong-disorder renormalization group has established an infinite-randomness fixed point (IRFP) with an infinite dynamic exponent, which describes the random-singlet (RS) state in random spin chains [19–27]. A characteristic feature of the 1D RS state is the drastic difference between the average and the typical spin correlations, which follow the r^{-2} power law and the exponential decay

respectively as a function of distance r due to the logarithmically broad probability distribution of spin correlation [23]. By extensive experimental studies on random spin chain compounds [28–34], recently RS behaviors have been reported in the compounds $BaCu_2(Si_{1-x}Ge_x)_2O_7$ and $Ba_5CuIr_3O_{12}$ [33,34]. In two dimensions (2D), it has been shown in experiment that increased disorder can also melt magnetic order and induce spin-liquid-like behaviors [35–39]. However, understanding the disorder effect in 2D frustrated systems is a longstanding challenge for theoretical study. Although the IRFP has been found in a few 2D systems [40–43], disorder-induced states in general frustrated Heisenberg models are quite elusive [44–46]. Recently, systematic exact diagonalization (ED) studies have unveiled a disordered phase driven by random couplings in various frustrated Heisenberg models, which is conjectured to be a 2D RS state [47–53]. The ED results of the dynamical and thermodynamic properties of this state qualitatively agree with the predictions of gapless spin liquids [47–54]. Nonetheless, the characteristic properties of the RS state such as the scaling behaviors of spin correlations have not been addressed and it is unresolved whether or not this disordered phase is indeed a RS state. A recent quantum Monte Carlo (QMC) study on the random J-Q model found a disordered state with the average spin correlation decaying algebraically as r^{-2}, which is proposed as the 2D analog of the RS state although the dynamic exponent is finite [55]. It is also conjectured that such a state should also exist in frustrated 2D Heisenberg spin systems with randomness [55], which,

*wuhanq3@mail.sysu.edu.cn
†donna.sheng1@csun.edu
‡shoushu.gong@buaa.edu.cn

however, has not been identified. Therefore, understanding the spin correlation behaviors is highly desired to identify the nature of the disorder-induced exotic state in 2D frustrated systems.

In this Letter, we use the large-scale density matrix renormalization group (DMRG) calculation to address the characteristic behaviors of spin correlations in a disorder-induced phase. We study the spin-1/2 square-lattice Heisenberg model with random nearest-neighbor (NN) J_1 and next-nearest-neighbor (NNN) J_2 couplings. This system may be considered as the preliminary description of the spin-liquid-like phase in the double perovskite $Sr_2CuTe_{1-x}W_xO_6$ [56–64], which realizes a simultaneous tuning of frustration and disorder by random Te-W cation mixing. The pure J_1-J_2 square Heisenberg model has a nonmagnetic phase near $J_2/J_1 = 0.5$ due to strong frustration [65–68]. With random couplings, a recent ED study has found evidence of a disordered phase and a possible spin-glass phase [52], without resolving the nature of the disordered phase. Based on the DMRG results, we identify a disordered phase without any magnetic order or spin-glass order [44] in the strong randomness regime. Furthermore, we unveil the $L_x^{-1/2}$ scaling of the spin-freezing parameter with system length L_x, the r^{-2} power-law decay of the average spin correlation, and the exponential decay of the typical spin correlation, which all agree with the corresponding behavior in the 1D RS state [23] and characterize the RS nature of this disordered state. The consistent r^{-2} behavior of average spin correlation also indicates that this state may belong to the same fixed point as the proposed RS state in the J-Q model, which demonstrates the robust universal behavior for such interacting and disorder systems. The vanished spin-freezing parameter in our model study implies that spin-glass order should be absent in $Sr_2CuTe_{1-x}W_xO_6$ at low temperature. Our results agree with the observations in the muon spin rotation (μSR) measurements of $Sr_2CuTe_{1-x}W_xO_6$, including the absent spin freezing for $x = 0.5$ at very low temperatures [56] and the large dynamic exponent supporting the intermediate RS phase [64].

The model with random J_1, J_2 couplings is defined as

$$H = \sum_{\langle ij \rangle} J_1(1 + \Delta\alpha_{ij})\mathbf{S}_i \cdot \mathbf{S}_j + \sum_{\langle\langle ij \rangle\rangle} J_2(1 + \Delta\beta_{ij})\mathbf{S}_i \cdot \mathbf{S}_j,$$

(1)

where α_{ij} and β_{ij} denote the random variables uniformly distributed in the interval $[-1, 1]$, and Δ controls the randomness strength of the interval $[J_i(1 - \Delta), J_i(1 + \Delta)]$ ($i = 1, 2$). We set $J_1 = 1.0$ and choose $\Delta/J_1 = 1.0$ to focus on the strong randomness case, as shown in Fig. 1. By using the DMRG with spin SU(2) symmetry [69,70], we simulate the system on the cylinder geometry with periodic boundary conditions along the circumference direction (y) and open boundary conditions along the axis direction (x), with L_y and L_x being the numbers of sites along the two directions. We study systems with L_y up to 10. To avoid edge effects, we choose $L_x = 2L_y$ in most calculations and compute physical quantities using the middle $L_y \times L_y$ subsystem, which is found valid by the agreement of our data with the QMC result. We keep 3000 SU(2) states [equivalent to about 12 000 U(1) states] to ensure the truncation error is smaller than 1×10^{-5}.
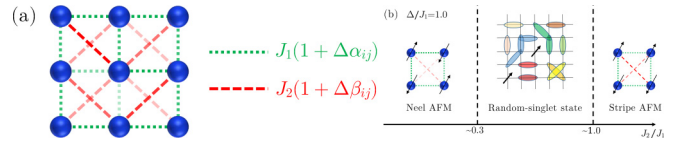

FIG. 1. Model Hamiltonian and quantum phase diagram of a spin-1/2 J_1-J_2 square-lattice Heisenberg model with random couplings. (a) The random NN J_1 (green bonds) and NNN J_2 (red bonds) couplings are uniformly distributed in the interval $\alpha_{ij}, \beta_{ij} \in [-1, 1]$. Δ is the strength of the randomness. (b) Quantum phase diagram of the model with growing J_2/J_1 and fixed $\Delta/J_1 = 1$, which shows a random-singlet phase between the Néel and stripe magnetic phase.

We take 100 (50) random samples for $L_y = 4, 6$ ($L_y = 8, 10$), which ensure a good sample average of the quantities; see Supplemental Material (SM) [71]. We use "$\langle \rangle$" and "[ ]" to represent quantum mechanical and stochastic averages, respectively.

Phase diagram and absent spin-glass order. We first determine the phase diagram of the system by computing magnetic order and spin-freezing parameters. We define the magnetic order parameter at the wave vector $\mathbf{k}$ as

$$m^2(\mathbf{k}) = \frac{1}{N_s^2} \sum_{i,j} [\langle \mathbf{S}_i \cdot \mathbf{S}_j \rangle] e^{i\mathbf{k} \cdot (\mathbf{r}_i - \mathbf{r}_j)},$$

(2)

where $N_s = L_y \times L_y$. The Néel and stripe magnetic order parameters can be defined as $m_N^2 = m^2(\pi, \pi)$ and $m_{str}^2 = [m^2(0, \pi) + m^2(\pi, 0)]/2$, where the results at $(0, \pi)$ and $(\pi, 0)$ are averaged to reduce the geometry effect. In Figs. 2(a) and 2(b), we show the polynomial size scaling of m_N^2 and m_{str}^2. For $J_2 = 0$, m_N^2 is smoothly extrapolated to 0.064 in the $N \to \infty$ limit, which agrees with the QMC data quite well [72] and shows the validity of our DMRG setup and calculation. With growing J_2, the Néel order seems to be melted at $J_2 \simeq 0.3$, where the Néel order parameters are smaller than those of the nonmagnetic state at $J_2 = 0.5$, $\Delta = 0$ [67,68]. For the larger J_2, m_{str}^2 becomes finite at $J_2 = 1.2, 1.5$ [see SM for the results of $m^2(0, \pi)$ and $m^2(\pi, 0)$ [71]], showing the stripe order survives from randomness. The strong average spin correlations at $J_2 = 1.2$ also support the emergent stripe order [71]. Based on the DMRG results, we identify an intermediate nonmagnetic phase.

We further explore a possible spin-glass phase in this nonmagnetic region [45,52]. Spin-glass order can be characterized by the spin-freezing parameter $\bar{q}$ [73] defined as

$$\bar{q} = \frac{1}{N_s} \sqrt{\sum_{ij} [\langle \mathbf{S}_i \cdot \mathbf{S}_j \rangle^2]}.$$

(3)

If spin orientations freeze, $\bar{q}$ would be nonzero in the thermodynamic limit. First, we show the size scaling of $\bar{q}$ vs L_x for a given L_y [$N_s = L_x \times L_y$ in Eq. (3)] in Figs. 2(c) and 2(d). On $L_y = 4, 6$ systems with large L_x, $\bar{q}$ clearly shows $L_x^{-1/2}$ scaling behavior, agreeing with that in the 1D RS state. We further study the decay behavior of $[\langle \mathbf{S}_i \cdot \mathbf{S}_j \rangle^2]$ as a function of $|i - j|$, which indeed supports this $L_x^{-1/2}$ scaling behavior [71]. We also notice that for any given L_x, $\bar{q}$ decreases with growing L_y, strongly indicating the absence of spin freezing in the large-size limit. To confirm this conclusion, we
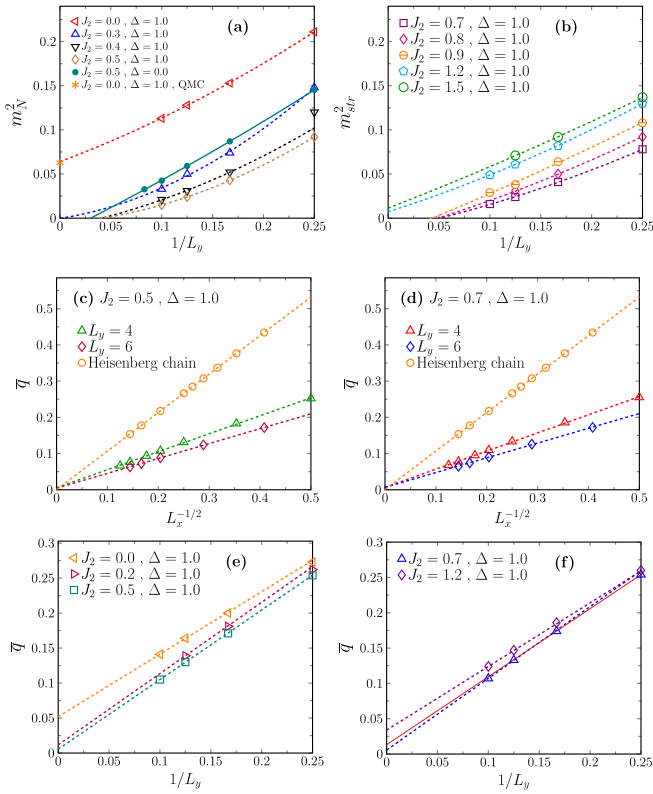
FIG. 2. Finite-size scaling of order parameters. (a) and (b) are the Néel (m_{N}^2) and stripe (m_{str}^2) order parameters vs $1/L_y$. For a comparison, we include the result of $J_2 = 0.5$, $\Delta = 0$ [67], which has been identified as a nonmagnetic state. The lines denote the polynomial fitting of the data up to the second order of $1/L_y$. The star symbol denotes the QMC result [72]. (c) and (d) are the spin-freezing parameter $\overline{q}$ vs $L_x^{-1/2}$ with $L_y = 4, 6$. The result of the 1D RS state of the Heisenberg chain is also shown. The good linear fittings indicate $\overline{q} \propto L_x^{-1/2}$. (e) and (f) are the spin-freezing parameter $\overline{q}$ vs $1/L_y$ obtained in the middle $L_y \times L_y$ subsystem. The dashed lines denote the linear fitting using the two largest-size data. The solid line in (f) shows the linear scaling of the small-size data with $L_y = 4$ and 6.

FIG. 3. Size scaling and distribution of spin correlation functions. (a) Log-log plot of the average absolute spin correlation vs L_y, which are defined for the largest-distance sites on the middle $L_y \times L_y$ subsystem as shown by the example in the inset. The dashed lines denote the fittings with $C_s(L_y) \sim L_y^{-2}$. (b) Log-log plot of the average absolute spin correlation $[|\langle \mathbf{S}_0 \cdot \mathbf{S}_r \rangle|]$ vs distance r along the axis direction of the cylinder. The reference site $\mathbf{S}_0$ is defined on the left-hand side of the middle $L_y \times L_y$ subsystem, and the site $\mathbf{S}_r$ is counted from the left- to right-hand side, as shown by the inset. The dashed lines denote the fittings with $C_s(r) \sim r^{-2}$. (c) and (d) show the data collapse of $P(x)$ vs $x = \ln(|C_{ij}|L_y^2)$ on different system sizes. (e) and (f) show the linear plot of $-[\ln |\langle \mathbf{S}_0 \cdot \mathbf{S}_r \rangle|]$ vs $r^{1/2}$.

also compute $\overline{q}$ in the middle $L_y \times L_y$ subsystem and analyze $\overline{q}$ vs $1/L_y$ as shown in Figs. 2(e) and 2(f). Since the $\overline{q}$ data decrease slightly faster than the linear behavior, we linearly extrapolate the results using the two largest-size data to reduce the finite-size effect. In the magnetic order phases, $\overline{q}$ goes to a finite value as expected. In the nonmagnetic region, we can also obtain a very small finite $\overline{q}$ that agrees with the ED conclusion [52] if we use linear scaling for small-size results, as shown by the solid line in Fig. 2(f). However, by fitting the larger-size data, $\overline{q}$ tends to vanish for $L_y \to \infty$, which agrees with the results shown in Figs. 2(c) and 2(d). The finite $\overline{q}$ in the ED calculation [52] should be owing to the larger-size effect.

Average and typical spin correlations. Next, we study the average and typical spin correlations to characterize this disordered phase. We analyze the average spin correlation in two ways. First, we consider the L_y dependence, which has been used in the study of the J-Q model [55]. We calculate the average absolute spin correlations that are defined for the largest-distance sites on the middle $L_y \times L_y$ subsystem,
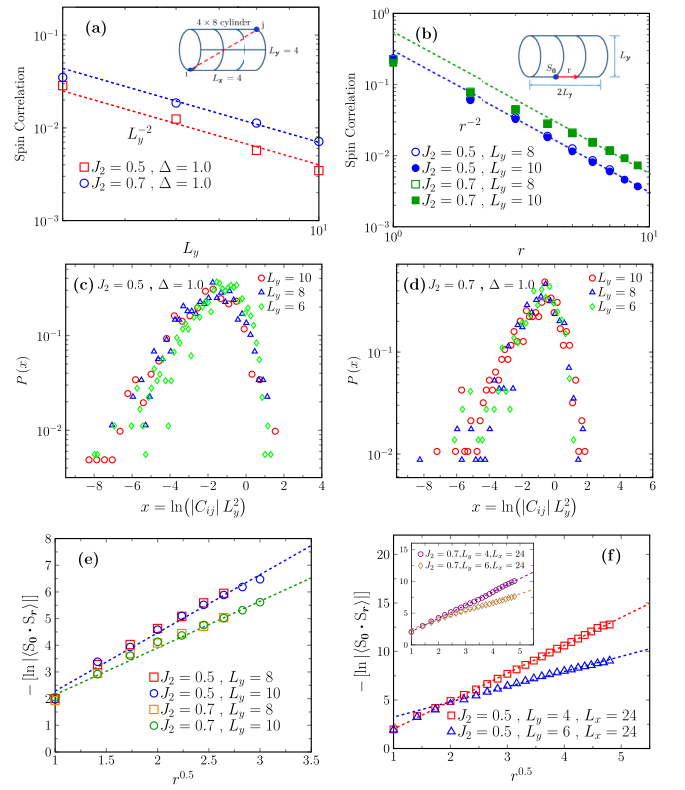
as illustrated in the inset of Fig. 3(a). The log-log plot of the average spin correlation versus L_y shows a power-law decay $C_s(L_y) \propto L_y^{-\alpha}$ with the exponent $\alpha \simeq 2$. This exponent agrees with that found in the RS state of the J-Q model [55]. Second, we study the average spin correlation decay along the x direction. To reduce the finite-size effects, we consider large systems with $L_y = 8, 10$ and $L_x = 2L_y$. We choose the reference site $\mathbf{S}_0$ on the left-hand side of the middle $L_y \times L_y$ subsystem and study the spin correlation decay $[|\langle \mathbf{S}_0 \cdot \mathbf{S}_r \rangle|]$ from the left- to right-hand side, as shown in Fig. 3(b). The average spin correlations shown here are very close, showing small finite-size effects and a consistent power-law decay $C_s(r) \propto r^{-2}$ (see SM for the smaller-size data and the consistent results for the weaker randomness strength, as well as preliminary results of the dimer-dimer correlationsbrk [71]).

We further investigate the probability distribution of the absolute spin correlations defined for the largest-distance sites in the middle $L_y \times L_y$ subsystem, denoted as $|C_{ij}|$. The probability $P(|C_{ij}|)$ vs $\ln |C_{ij}|$ on different sizes becomes broader

with growing L_y [71], which agrees with the decrease of $C_s(L_y)$. To eliminate the finite-size effects in the analysis, we define a new scaling variable $x = \ln(|C_{ij}|L_y^2)$ and plot $P(x)$ vs x in Figs. 3(c) and 3(d). Any distribution $P(x)$ with data collapse for different L_y must lead to the power-law decay of the average spin correlation

$$C_s(L_y) = \int_0^\infty dx P(x) \frac{e^x}{L_y^2} \propto L_y^{-2}. \tag{4}$$

Thus, the good data collapse in Figs. 3(c) and 3(d) further supports the power-law decay of $C_s(L_y)$ found in Fig. 3(a).

The logarithmically broad distribution of spin correlations may lead to the exponential decay of the typical spin correlation defined as $\exp[\ln|\langle \mathbf{S}_0 \cdot \mathbf{S}_r \rangle|]$. In the 1D RS state, the exponential typical spin correlation can be equivalently described as $-[\ln|\langle \mathbf{S}_0 \cdot \mathbf{S}_r \rangle|] \propto r^{1/2}$ [23]. We show the linear plot of $-[\ln|\langle \mathbf{S}_0 \cdot \mathbf{S}_r \rangle|]$ vs $r^{1/2}$ in Figs. 3(e) and 3(f). On both the $L_y = 8, 10, L_x = 2L_y$ systems and the $L_y = 4, 6$ cylinders with large L_x, $-[\ln|\langle \mathbf{S}_0 \cdot \mathbf{S}_r \rangle|]$ follows the linear scaling with $r^{1/2}$ quite well. We also analyze $-[\ln|\langle \mathbf{S}_0 \cdot \mathbf{S}_r \rangle|]$ vs r using the log-log manner [71], which shows good power-law dependence and the slope gives a power exponent very close to $1/2$, supporting the results in Figs. 3(e) and 3(f). Therefore, our results unveil the characteristic behaviors of spin correlations, which suggest the RS nature of this disordered phase.

Excitation gaps and microscopic clusters. A previous ED study found the vanished spin gap in the disordered phase [52]. To further unveil the properties of excitations, we separately compute spin-triplet and spin-singlet gaps by using ED. Compared with the results in the Néel phase, both triplet and singlet gaps in the disordered phase decrease, as shown in Figs. 4(a) and 4(b), showing the vanished gaps in the thermodynamic limit [74]. In particular, while the finite-size data of the triplet gap slightly decrease, the singlet gap is strongly suppressed.

In the presence of disorder, local clusters may form in microscopic scale. A recent ED study has found three types of clusters in random spin systems, including an isolated dimer, resonating-dimer cluster, and orphan spin [53], which should be helpful for understanding low-energy excitations. We extend such an analysis in different phases based on the DMRG results. For each sample on the $L_x = 2L_y$ cylinder, we collect all the correlations $\langle \mathbf{S}_i \cdot \mathbf{S}_j \rangle$ in the middle $L_y \times L_y$ subsystem. We define the isolated dimer as a singlet pair with strong correlation, the resonating-dimer cluster as a cluster with more than two strongly coupled spins, and the orphan spin as the one weakly coupled to other spins (see SM [71] and Ref. [53] for the procedure to obtain the covering of clusters). One example of the covering is shown in Fig. 4(c). For each random sample we compute the ratios for the different types of clusters and then take their sample averages, as shown in Fig. 4(d). In the three quantum phases, the dominant cluster is always the isolated dimer due to strong bond randomness, and the ratio of the orphan spin varies slightly. A feature in the disordered state is the less resonating dimers compared with magnetic states. In the RS picture, the triplet excitations are related to breaking dimers. The broad distribution of bond couplings causes a decrease of the triplet excitation gap. For singlet excitations which are related to spin flip in magnetic
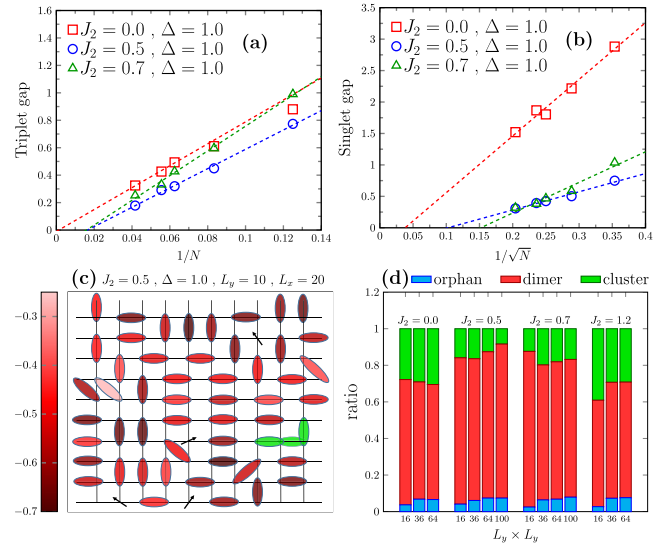

FIG. 4. Finite-size scaling of gaps and distributions of microscopic clusters. (a) and (b) are the gaps obtained from the ED calculation. $N = 8, 12, 16, 18, 24$ is the total site number. The linear fitting curves are guides to the eye. (c) The covering of isolated dimers (the red ellipse), resonating-dimer clusters (the connected green ellipses), and orphan spins (the arrow) on the lattice with a given random sample. The gradation of the red color corresponds to the strength of the bond correlation $\langle \mathbf{S}_i \cdot \mathbf{S}_j \rangle$. (d) The ratios of the different clusters in different quantum phases. We analyze the data from the middle $L_y \times L_y$ subsystem.

phases, in the RS state such excitations could be driven by the diffusion of orphan spins [53], which may account for the strongly suppressed singlet gap in Fig. 4(b). Due to the size limit, here we only focus on the features of the small clusters. The collective properties on a larger length scale need future study beyond the present system size.

Conclusion and discussion. We have studied the ground states of a spin-$1/2$ square Heisenberg model with random J_1, J_2 couplings in the strong disorder regime by using a large-scale DMRG calculation. With growing J_2, we find a gapless phase without any magnetic order or spin-glass order. We identify the characteristic size-scaling behaviors of spin correlations in this state, including the $L_x^{-1/2}$ scaling of the spin-freezing parameter with a system length L_x, the r^{-2} power-law decay of the average spin correlation, and the exponential decay of the typical spin correlation. Although the RS state of a generic 2D system is not well understood, our results strongly suggest this disordered state as the 2D analog of the 1D RS state. The same scaling behavior of an average spin correlation in this frustrated model and the J-Q model also suggests the same fixed point of the states in these different systems. For further study, the dynamic exponent may be explored by a tensor network simulation at finite temperature [75,76] or an analysis of the excitation gap distribution (a rough estimation of the dynamic exponent from ED gap data is shown in SM [71]).

For $Sr_2CuTe_{1-x}W_xO_6$, spin freezing has been excluded for $x = 0.5$ [56], which agrees with our results. For more mixing ratios, the μSR measurement has identified a large

dynamic exponent supporting the intermediate RS phase in $Sr_2CuTe_{1-x}W_xO_6$ [64]. At last, we emphasize that this 2D RS state should be considered as the preliminary understanding of the spin-liquid-like state in $Sr_2CuTe_{1-x}W_xO_6$, since the bond randomness in our study is a simplified picture to describe the random substitution in $Sr_2CuTe_{1-x}W_xO_6$ [64]. We leave the more realistic modeling of the material to future study.

[1] C. Lacroix, P. Mendels, and F. Mila, Introduction to Frustrated Magnetism Materials, Experiments, Theory, Springer Series in Solid-State Science, Vol. 164 (Springer, 2011).

[2] L. Balents, Spin liquids in frustrated magnets, Nature (London) **464**, 199 (2010).

[3] L. Savary and L. Balents, Quantum spin liquids: A review, Rep. Prog. Phys. **80**, 016502 (2017).

[4] M. R. Norman, Colloquium: Herbertsmithite and the search for the quantum spin liquid, Rev. Mod. Phys. **88**, 041002 (2016).

[5] Y. Zhou, K. Kanoda, and T.-K. Ng, Quantum spin liquid states, Rev. Mod. Phys. **89**, 025003 (2017).

[6] X. G. Wen, Mean-field theory of spin-liquid states with finite energy gap and topological orders, Phys. Rev. B **44**, 2664 (1991).

[7] N. Read and S. Sachdev, Large-N Expansion for Frustrated Quantum Antiferromagnets, Phys. Rev. Lett. **66**, 1773 (1991).

[8] X. Chen, Z.-C. Gu, and X.-G. Wen, Local unitary transformation, long-range quantum entanglement, wave function renormalization, and topological order, Phys. Rev. B **82**, 155138 (2010).

[9] A. Kitaev, Anyons in an exactly solved model and beyond, Ann. Phys. **321**, 2 (2006).

[10] B. Fåk, E. Kermarrec, L. Messio, B. Bernu, C. Lhuillier, F. Bert, P. Mendels, B. Koteswararao, F. Bouquet, J. Ollivier, A. D. Hillier, A. Amato, R. H. Colman, and A. S. Wills, Kapellasite: A Kagome Quantum Spin Liquid with Competing Interactions, Phys. Rev. Lett. **109**, 037208 (2012).

[11] Y. Shimizu, K. Miyagawa, K. Kanoda, M. Maesato, and G. Saito, Spin Liquid State in an Organic Mott Insulator with a Triangular Lattice, Phys. Rev. Lett. **91**, 107001 (2003).

[12] S. Yamashita, Y. Nakazawa, M. Oguni, Y. Oshima, H. Nojiri, Y. Shimizu, K. Miyagawa, and K. Kanoda, Thermodynamic properties of a spin-1/2 spin-liquid state in a κ-type organic salt, Nat. Phys. **4**, 459 (2008).

[13] Y. Li, H. Liao, Z. Zhang, S. Li, F. Jin, L. Ling, L. Zhang, Y. Zou, L. Pi, Z. Yang, J. Wang, Z. Wu, and Q. Zhang, Gapless quantum spin liquid ground state in the two-dimensional spin-1/2 triangular antiferromagnet $YbMgGaO_4$, Sci. Rep. **5**, 16419 (2015).

[14] Y. Li, G. Chen, W. Tong, L. Pi, J. Liu, Z. Yang, X. Wang, and Q. Zhang, Rare-Earth Triangular Lattice Spin Liquid: A Single-Crystal Study of $YbMgGaO_4$, Phys. Rev. Lett. **115**, 167203 (2015).

[15] Y. Shen, Y.-D. Li, H. Wo, Y. Li, S. Shen, B. Pan, Q. Wang, H. C. Walker, P. Steffens, M. Boehm, Y. Hao, D. L. Quintero-Castro, L. W. Harriger, M. D. Frontzek, L. Hao, S. Meng, Q. Zhang, G. Chen, and J. Zhao, Evidence for a spinon Fermi surface in a triangular-lattice quantum-spin-liquid candidate, Nature (London) **540**, 559 (2016).

[16] J. A. M. Paddison, M. Daum, Z. Dun, G. Ehlers, Y. Liu, M. B. Stone, H. Zhou, and M. Mourigal, Continuous excitations of the triangular-lattice quantum spin liquid $YbMgGaO_4$, Nat. Phys. **13**, 117 (2017).

[17] D. E. Freedman, T. H. Han, A. Prodi, P. Muller, Q.-Z. Huang, Y.-S. Chen, S. M. Webb, Y. S. Lee, T. M. McQueen, and D. G. Nocera, Site specific x-ray anomalous dispersion of the geometrically frustrated kagome magnet, herbertsmithite, $ZnCu_3(OH)_6Cl_2$, J. Am. Chem. Soc. **132**, 16185 (2010).

[18] M. Zhu, D. Do, C. R. Dela Cruz, Z. Dun, H. D. Zhou, S. D. Mahanti, and X. Ke, Tuning the Magnetic Exchange via a Control of Orbital Hybridization in $Cr_2(Te_{1-x}W_x)O_6$, Phys. Rev. Lett. **113**, 076406 (2014).

[19] S.-k. Ma, C. Dasgupta, and C.-k. Hu, Random Antiferromagnetic Chain, Phys. Rev. Lett. **43**, 1434 (1979).

[20] C. Dasgupta and S.-k. Ma, Low-temperature properties of the random Heisenberg antiferromagnetic chain, Phys. Rev. B **22**, 1305 (1980).

[21] R. N. Bhatt and P. A. Lee, Scaling Studies of Highly Disordered Spin-$\frac{1}{2}$ Antiferromagnetic Systems, Phys. Rev. Lett. **48**, 344 (1982).

[22] D. S. Fisher, Random Transverse Field Ising Spin Chains, Phys. Rev. Lett. **69**, 534 (1992).

[23] D. S. Fisher, Random antiferromagnetic quantum spin chains, Phys. Rev. B **50**, 3799 (1994).

[24] D. S. Fisher, Critical behavior of random transverse-field Ising spin chains, Phys. Rev. B **51**, 6411 (1995).

[25] R. Mélin, Y.-C. Lin, P. Lajkó, H. Rieger, and F. Iglói, Strongly disordered spin ladders, Phys. Rev. B **65**, 104415 (2002).

[26] G. Refael, S. Kehrein, and D. S. Fisher, Spin reduction transition in spin-$\frac{3}{2}$ random Heisenberg chains, Phys. Rev. B **66**, 060402(R) (2002).

[27] Y.-R. Shu, D.-X. Yao, C.-W. Ke, Y.-C. Lin, and A. W. Sandvik, Properties of the random-singlet phase: From the disordered Heisenberg chain to an amorphous valence-bond solid, Phys. Rev. B **94**, 174442 (2016).

[28] L. N. Bulaevski, A. V. Zvarykina, Yu. S. Karimov, R. B. Lyubovskii, and I. F. Shchegolev, Magnetic properties of linear conducting chains, Sov. Phys. JETP **35**, 384 (1972).

[29] T. N. Nguyen, P. A. Lee, and H.-C. zur Loye, Design of a random quantum spin chain paramagnet: $Sr_3CuPt_{0.5}Ir_{0.5}O_6$, Science **271**, 489 (1996).

[30] A. Niazi, E.V. Sampathkumaran, P.L. Paulose, D. Eckert, A. Handstein, and K.-H. Müller, Sr_3CuIrO_6, a spin-chain compound with random ferromagnetic-antiferromagnetic interactions, Solid State Commun. **120**, 11 (2001).

[31] T. Nakamura, Antiferromagnetic order in an ferromagnetic-antiferromagnetic random alternating quantum spin chain: $(CH_3)_2CHNH_3Cu(Cl_xBr_{1-x})_3$, J. Phys. Soc. Jpn. **72**, 789 (2003).

[32] T. Shiroka, F. Casola, V. Glazkov, A. Zheludev, K. Prša, H.-R. Ott, and J. Mesot, Distribution of NMR Relaxations in a Random Heisenberg Chain, Phys. Rev. Lett. **106**, 137202 (2011).

[33] T. Shiroka, F. Eggenschwiler, H.-R. Ott, and J. Mesot, From order to randomness: Onset and evolution of the random-singlet state in bond-disordered $BaCu_2(Si_{1-x}Ge_x)_2O_7$ spin-chain compounds, Phys. Rev. B **99**, 035116 (2019).

[34] P. A. Volkov, C.-J. Won, D. I. Gorbunov, J. Kim, M. Ye, H.-S. Kim, J. H. Pixley, S.-W. Cheong, and G. Blumberg, Random singlet state in $Ba_5CuIr_3O_{12}$ single crystals, Phys. Rev. B **101**, 020406(R) (2020).

[35] T. Ono, H. Tanaka, T. Nakagomi, O. Kolomiyets, H. Mitamura, F. Ishikawa, T. Goto, K. Nakajima, A. Oosawa, Y. Koike, K. Kakurai, J. Klenke, P. Smeibidle, M. Meiner, and H. Aruga Katori, Phase transitions and disorder effects in pure and doped frustrated quantum antiferromagnet Cs_2CuBr_4, J. Phys. Soc. Jpn. **74**, 135 (2005).

[36] K. Katayama, N. Kurita, and H. Tanaka, Quantum phase transition between disordered and ordered states in the spin-$\frac{1}{2}$ kagome lattice antiferromagnet $(Rb_{1-x}Cs_x)_2Cu_3SnF_{12}$, Phys. Rev. B **91**, 214429 (2015).

[37] T. Furukawa, K. Miyagawa, T. Itou, M. Ito, H. Taniguchi, M. Saito, S. Iguchi, T. Sasaki, and K. Kanoda, Quantum Spin Liquid Emerging from Antiferromagnetic Order by Introducing Disorder, Phys. Rev. Lett. **115**, 077001 (2015).

[38] H. Yamaguchi, M. Okada, Y. Kono, S. Kittaka, T. Sakakibara, T. Okabe, Y. Iwasaki, and Y. Hosokoshi, Randomness-induced quantum spin liquid on honeycomb lattice, Sci. Rep. **7**, 16144 (2017).

[39] L. Savary and L. Balents, Disorder-Induced Quantum Spin Liquid in Spin Ice Pyrochlores, Phys. Rev. Lett. **118**, 087203 (2017).

[40] O. Motrunich, S.-C. Mau, D. A. Huse, and D. S. Fisher, Infinite-randomness quantum Ising critical fixed points, Phys. Rev. B **61**, 1160 (2000).

[41] István A. Kovács and F. Iglói, Infinite-disorder scaling of random quantum magnets in three and higher dimensions, Phys. Rev. B **83**, 174207 (2011).

[42] T. Vojta, A. Farquhar, and J. Mast, Infinite-randomness critical point in the two-dimensional disordered contact process, Phys. Rev. E **79**, 011111 (2009).

[43] T. Vojta, C. Kotabage, and J. A. Hoyos, Infinite-randomness quantum critical points induced by dissipation, Phys. Rev. B **79**, 024401 (2009).

[44] J. Oitmaa and O. P. Sushkov, Two-Dimensional Randomly Frustrated Spin-1/2 Heisenberg Model, Phys. Rev. Lett. **87**, 167206 (2001).

[45] Y.-C. Lin, R. Mélin, H. Rieger, and F. Iglói, Low-energy fixed points of random Heisenberg models, Phys. Rev. B **68**, 024424 (2003).

[46] I. Kimchi, J. P. Sheckelton, T. M. McQueen, and P. A. Lee, Scaling and data collapse from local moments in frustrated disordered quantum spin systems, Nat. Commun. **9**, 4367 (2018).

[47] K. Watanabe, H. Kawamura, H. Nakano, and T. Sakai, Quantum spin-liquid behavior in the spin-1/2 random Heisenberg antifer-

[48] H. Kawamura, K. Watanabe, and T. Shimokawa, Quantum spin-liquid behavior in the spin-1/2 random-bond Heisenberg antiferromagnet on the kagome lattice, J. Phys. Soc. Jpn. **83**, 103704 (2014).

[49] T. Shimokawa, K. Watanabe, and H. Kawamura, Static and dynamical spin correlations of the $S = \frac{1}{2}$ random-bond antiferromagnetic Heisenberg model on the triangular and kagome lattices, Phys. Rev. B **92**, 134407 (2015).

[50] K. Uematsu and H. Kawamura, Randomness-induced quantum spin liquid behavior in the $S = 1/2$ random J_1-J_2 Heisenberg antiferromagnet on the honeycomb lattice, J. Phys. Soc. Jpn. **86**, 044704 (2017).

[51] H.-Q. Wu, S.-S. Gong, and D. N. Sheng, Randomness-induced spin-liquid-like phase in the spin-$\frac{1}{2}$ J_1-J_2 triangular Heisenberg model, Phys. Rev. B **99**, 085141 (2019).

[52] K. Uematsu and H. Kawamura, Randomness-induced quantum spin liquid behavior in the $S = \frac{1}{2}$ random J_1-J_2 Heisenberg antiferromagnet on the square lattice, Phys. Rev. B **98**, 134427 (2018).

[53] H. Kawamura and K. Uematsu, Nature of the randomness-induced quantum spin liquids in two dimensions, J. Phys.: Condens. Matter **31**, 504003 (2019).

[54] R. R. P. Singh, Valence Bond Glass Phase in Dilute Kagome Antiferromagnets, Phys. Rev. Lett. **104**, 177203 (2010).

[55] L. Liu, H. Shao, Y.-C. Lin, W. Guo, and A. W. Sandvik, Random-Singlet Phase in Disordered Two-Dimensional Quantum Magnets, Phys. Rev. X **8**, 041040 (2018).

[56] O. Mustonen, S. Vasala, E. Sadrollahi, K. P. Schmidt, C. Baines, H. C. Walker, I. Terasaki, F. J. Litterst, E. Baggio-Saitovitch, and M. Karppinen, Spin-liquid-like state in a spin-1/2 square-lattice antiferromagnet perovskite induced by d^{10}–d^0 cation mixing, Nat. Commun. **9**, 1085 (2018).

[57] O. Mustonen, S. Vasala, K. P. Schmidt, E. Sadrollahi, H. C. Walker, I. Terasaki, F. J. Litterst, E. Baggio-Saitovitch, and M. Karppinen, Tuning the $S = 1/2$ square-lattice antiferromagnet $Sr_2Cu(Te_{1-x}W_x)O_6$ from Néel order to quantum disorder to columnar order, Phys. Rev. B **98**, 064411 (2018).

[58] M. Watanabe, N. Kurita, H. Tanaka, W. Ueno, K. Matsui, and T. Goto, Valence-bond-glass state with a singlet gap in the spin-$\frac{1}{2}$ square-lattice random J_1-J_2 Heisenberg antiferromagnet $Sr_2CuTe_{1-x}W_xO_6$, Phys. Rev. B **98**, 054422 (2018).

[59] S. Vasala, M. Avdeev, S. Danilkin, O. Chmaissem, and M. Karppinen, Magnetic structure of Sr_2CuCO_6, J. Phys.: Condens. Matter **26**, 496001 (2014).

[60] P. Babkevich, V. M. Katukuri, B. Fåk, S. Rols, T. Fennell, D. Pajić, H. Tanaka, T. Pardini, R. R. P. Singh, A. Mitrushchenkov, O. V. Yazyev, and H. M. Rønnow, Magnetic Excitations and Electronic Interactions in Sr_2CuTeO_6: A Spin-1/2 Square Lattice Heisenberg Antiferromagnet, Phys. Rev. Lett. **117**, 237203 (2016).

[61] H. C. Walker, O. Mustonen, S. Vasala, D. J. Voneshen, M. D. Le, D. T. Adroja, and M. Karppinen, Spin wave excitations in the tetragonal double perovskite Sr_2CuWO_6, Phys. Rev. B **94**, 064411 (2016).

[62] T. Koga, N. Kurita, M. Avdeev, S. Danilkin, T. J. Sato, and H. Tanaka, Magnetic structure of the $S = \frac{1}{2}$ quasi-two-dimensional square-lattice Heisenberg antiferromagnet Sr_2CuTeO_6, Phys. Rev. B **93**, 054426 (2016).

[63] V. M. Katukuri, P. Babkevich, O. Mustonen, H. C. Walker, B. Fåk, S. Vasala, M. Karppinen, H. M. Rønnow, and O. V. Yazyev, Exchange Interactions Mediated by Nonmagnetic Cations in Double Perovskites, Phys. Rev. Lett. **124**, 077202 (2020).

[64] W. Hong, L. Liu, C. Liu, X. Ma, A. Koda, X. Li, J. Song, W. Yang, J. Yang, P. Cheng, H. Zhang, W. Bao, X. Ma, D. Chen, K. Sun, W. Guo, H. Luo, A. W. Sandvik, and S. Li, Extreme Suppression of Antiferromagnetic Order and Critical Scaling in a Two-Dimensional Random Quantum Magnet, Phys. Rev. Lett. **126**, 037201 (2021).

[65] P. Chandra and B. Doucot, Possible spin-liquid state at large S for the frustrated square Heisenberg lattice, Phys. Rev. B **38**, 9335(R) (1988).

[66] S. Sachdev and R. N. Bhatt, Bond-operator representation of quantum spins: Mean-field theory of frustrated quantum Heisenberg antiferromagnets, Phys. Rev. B **41**, 9323 (1990).

[67] S.-S. Gong, W. Zhu, D. N. Sheng, O. I. Motrunich, and M. P. A. Fisher, Plaquette Ordered Phase and Quantum Phase Diagram in the Spin-$\frac{1}{2}$ J_1-J_2 Square Heisenberg Model, Phys. Rev. Lett. **113**, 027201 (2014).

[68] W.-Y. Liu, S.-S. Gong, Y.-B. Li, D. Poilblanc, W.-Q. Chen, and Z.-C. Gu, Gapless quantum spin liquid and global phase diagram of the spin-1/2 J_1-J_2 square antiferromagnetic Heisenberg model, Sci. Bull. **67**, 1034 (2022).

[69] S. R. White, Density Matrix Formulation for Quantum Renormalization Groups, Phys. Rev. Lett. **69**, 2863 (1992).

[70] I. P. McCulloch and M. Gulácsi, The non-Abelian density matrix renormalization group algorithm, Europhys. Lett. **57**, 852 (2002).

[71] See Supplemental Material at http://link.aps.org/supplemental/10.1103/PhysRevB.107.L020407 for more details.

[72] N. Laflorencie, S. Wessel, A. Läuchli, and H. Rieger, Random-exchange quantum Heisenberg antiferromagnets on a square lattice, Phys. Rev. B **73**, 060403(R) (2006).

[73] K. Binder and A. P. Young, Spin glasses: Experimental facts, theoretical concepts, and open questions, Rev. Mod. Phys. **58**, 801 (1986).

[74] Since the Néel and stripe antiferromagnetic phase break SU(2) symmetry spontaneously in the thermodynamic limit, the energy spectrum has the Anderson tower of states on finite-size systems. With growing system size, the tower of states levels scale with $1/N$ to the ground state, and the low-energy magnon excitations scale with $1/\sqrt{N}$, where N is the total number of sites. Therefore, we scale the triplet gap with $1/N$ and singlet gap with $1/\sqrt{N}$.

[75] B.-B. Chen, L. Chen, Z. Chen, W. Li, and A. Weichselbaum, Exponential Thermal Tensor Network Approach for Quantum Lattice Models, Phys. Rev. X **8**, 031082 (2018).

[76] H. Li, Y. D. Liao, B.-B. Chen, X.-T. Zeng, X.-L. Sheng, Y. Qi, Z. Y. Meng, and W. Li, Kosterlitz-Thouless melting of magnetic order in the triangular quantum Ising material TmMgGaO$_4$, Nat. Commun. **11**, 1111 (2020).